

9-2013

## Complex reflection coefficients of p- and s-polarized light at the pseudo-Brewster angle of a dielectric–conductor interface

Rasheed M.A. Azzam

*University of New Orleans, razzam@uno.edu*

Follow this and additional works at: [https://scholarworks.uno.edu/ee\\_facpubs](https://scholarworks.uno.edu/ee_facpubs)



Part of the [Electrical and Computer Engineering Commons](#), and the [Optics Commons](#)

---

### Recommended Citation

R. M. A. Azzam, "Complex reflection coefficients of p- and s-polarized light at the pseudo-Brewster angle of a dielectric–conductor interface," *J. Opt. Soc. Am. A* 30, 1975-1979 (2013)

This Article is brought to you for free and open access by the Department of Electrical Engineering at ScholarWorks@UNO. It has been accepted for inclusion in Electrical Engineering Faculty Publications by an authorized administrator of ScholarWorks@UNO. For more information, please contact [scholarworks@uno.edu](mailto:scholarworks@uno.edu).

# Complex reflection coefficients of $p$ - and $s$ -polarized light at the pseudo-Brewster angle of a dielectric–conductor interface

R. M. A. Azzam

Department of Electrical Engineering, University of New Orleans, New Orleans, Louisiana 70148, USA  
(razzam@uno.edu)

Received July 23, 2013; revised August 15, 2013; accepted August 16, 2013;

posted August 16, 2013 (Doc. ID 194457); published September 10, 2013

The complex Fresnel reflection coefficients  $r_p$  and  $r_s$  of  $p$ - and  $s$ -polarized light and their ratio  $\rho = r_p/r_s$  at the pseudo-Brewster angle (PBA)  $\phi_{pB}$  of a dielectric–conductor interface are evaluated for all possible values of the complex relative dielectric function  $\varepsilon = |\varepsilon| \exp(-j\theta) = \varepsilon_r - j\varepsilon_i$ ,  $\varepsilon_i > 0$  that share the same  $\phi_{pB}$ . Complex-plane trajectories of  $r_p$ ,  $r_s$ , and  $\rho$  at the PBA are presented at discrete values of  $\phi_{pB}$  from  $5^\circ$  to  $85^\circ$  in equal steps of  $5^\circ$  as  $\theta$  is increased from  $0^\circ$  to  $180^\circ$ . It is shown that for  $\phi_{pB} > 70^\circ$  (high-reflectance metals in the IR)  $r_p$  at the PBA is essentially pure negative imaginary and the reflection phase shift  $\delta_p = \arg(r_p) \approx -90^\circ$ . In the domain of fractional optical constants (vacuum UV or light incidence from a high-refractive-index immersion medium)  $0 < \phi_{pB} < 45^\circ$  and  $r_p$  is pure real negative ( $\delta_p = \pi$ ) when  $\theta = \tan^{-1}(\sqrt{\cos(2\phi_{pB})})$ , and the corresponding locus of  $\varepsilon$  in the complex plane is obtained. In the limit of  $\varepsilon_i = 0$ ,  $\varepsilon_r < 0$  (interface between a dielectric and plasmonic medium) the total reflection phase shifts  $\delta_p$ ,  $\delta_s$ ,  $\Delta = \delta_p - \delta_s = \arg(\rho)$  are also determined as functions of  $\phi_{pB}$ . © 2013 Optical Society of America

OCIS codes: (120.5700) Reflection; (240.0240) Optics at surfaces; (240.2130) Ellipsometry and polarimetry; (260.0260) Physical optics; (260.3910) Metal optics; (260.5430) Polarization.

<http://dx.doi.org/10.1364/JOSAA.30.001975>

## 1. INTRODUCTION

A salient feature of the reflection of collimated monochromatic  $p$  (TM)-polarized light at a planar interface between a transparent medium of incidence (dielectric) and an absorbing medium of refraction (conductor) is the appearance of a reflectance minimum at the pseudo-Brewster angle (PBA)  $\phi_{pB}$ . If the medium of refraction is also transparent, the minimum reflectance is zero and  $\phi_{pB}$  reverts back to the usual Brewster angle  $\phi_B = \tan^{-1} n = \tan^{-1} \sqrt{\varepsilon_r}$ . The PBA  $\phi_{pB}$  is determined by the complex relative dielectric function  $\varepsilon = \varepsilon_1/\varepsilon_0 = \varepsilon_r - j\varepsilon_i$ ,  $\varepsilon_i > 0$ , where  $\varepsilon_0$  and  $\varepsilon_1$  are the real and complex permittivities of the dielectric and conductor, respectively, by solving a cubic equation in  $u = \sin^2 \phi_{pB}$  [1–5]. Measurement of  $\phi_{pB}$  and of reflectance at that angle or at normal incidence enables the determination of complex  $\varepsilon$  [1,6–9]. It is also possible to determine  $\varepsilon$  of an optically thick absorbing film from two PBAs measured in transparent ambient and substrate media that sandwich the thick film [10]. Reflection at the PBA has also had other interesting applications [11,12].

For light reflection at any angle of incidence  $\phi$  the complex-amplitude Fresnel reflection coefficients (see, e.g., [13]) of the  $p$  and  $s$  polarizations are given by

$$r_p = \frac{\varepsilon \cos \phi - (\varepsilon - \sin^2 \phi)^{1/2}}{\varepsilon \cos \phi + (\varepsilon - \sin^2 \phi)^{1/2}}, \quad (1)$$

$$r_s = \frac{\cos \phi - (\varepsilon - \sin^2 \phi)^{1/2}}{\cos \phi + (\varepsilon - \sin^2 \phi)^{1/2}}. \quad (2)$$

All possible values of complex  $\varepsilon = (\varepsilon_r, \varepsilon_i)$  that share the same  $\phi_{pB}$  are generated by using the following algorithm [8,14]:

$$\varepsilon_r = |\varepsilon| \cos \theta, \quad \varepsilon_i = |\varepsilon| \sin \theta, \quad (3)$$

$$\begin{aligned} |\varepsilon| &= \ell \cos(\zeta/3), \\ \ell &= 2u \left(1 - \frac{2}{3}u\right)^{1/2} / (1-u), \\ \zeta &= \cos^{-1} \left[ -(1-u) \cos \theta / \left(1 - \frac{2}{3}u\right)^{3/2} \right], \\ u &= \sin^2 \phi_{pB}, \\ 0 &\leq \theta \leq 180^\circ. \end{aligned} \quad (4)$$

As  $\theta$  is increased from  $0^\circ$  to  $180^\circ$ , the minimum reflectance  $|r_p|_{\min}$  at a given  $\phi_{pB}$  increases monotonically from 0 to 1 [15] and also as is evident in Fig. 1 of Section 2.

In this paper, loci of all possible values of complex  $r_p = |r_p| \exp(j\delta_p)$ ,  $r_s = |r_s| \exp(j\delta_s)$ , and  $\rho = r_p/r_s = |\rho| \exp(j\Delta)$  at the PBA are determined at discrete values of  $\phi_{pB}$  from  $5^\circ$  to  $85^\circ$  in equal steps of  $5^\circ$  and as  $\theta = -\arg(\varepsilon)$  covers the full range  $0^\circ \leq \theta \leq 180^\circ$ . These results are presented in Sections 2, 3, and 4, respectively, and lead to interesting conclusions. In particular, questions related to phase shifts that accompany the reflection of  $p$ - and  $s$ -polarized light at the PBA (e.g., [12]) are settled. Section 5 summarizes the essential conclusions of this paper.

## 2. COMPLEX REFLECTION COEFFICIENT OF THE *p* POLARIZATION AT THE PBA

Figure 1 shows the loci of complex  $r_p$  as  $\theta$  increases from  $0^\circ$  to  $180^\circ$  at constant values of  $\phi_{pB}$  from  $5^\circ$  to  $85^\circ$  in equal steps of  $5^\circ$ . All constant- $\phi_{pB}$  contours begin at the origin  $O$  ( $\theta = 0$ ) as a common point, that represents zero reflection at an ideal Brewster angle, and end on the  $90^\circ$  arc of the unit circle in the third quadrant (shown as a dotted line) that represents total reflection  $|r_p| = 1$  at  $\theta = 180^\circ$  ( $\epsilon_i = 0, \epsilon_r < 0$ ). A quick conclusion from Fig. 1 is that for  $\phi_{pB} > 70^\circ$  (high-reflectance metals)  $r_p$  at the PBA is essentially pure negative imaginary, and  $\delta_p \approx -90^\circ$ .

In Fig. 1 the constant- $\phi_{pB}$  contours of  $r_p$  for  $0 < \phi_{pB} < 45^\circ$  spill over into a limited range of the second quadrant of the complex plane and each contour intersects the negative real axis. In Appendix A it is shown that  $\theta$  at the point of intersection, where  $\delta_p = \arg(r_p) = \pi$ , is given by the remarkably simple formula

$$\theta(\delta_p = \pi) = \tan^{-1}\left(\sqrt{\cos(2\phi_{pB})}\right). \quad (5)$$

A graph of this function of Eq. (5) is shown in Fig. 2.

The locus of complex  $\epsilon$  such that  $\delta_p = \arg(r_p) = \pi$  at the PBA [as determined by Eqs. (3)–(5)] falls in the domain of fractional optical constants and is shown in Fig. 3. The end points  $(0, 0)$  and  $(1, 0)$  of this trajectory correspond to  $\phi_{pB} = 0$  and  $45^\circ$ , respectively. At  $\epsilon = (0.6, 0.3)$ , a point that falls exactly on the curve very near to its peak,  $\phi_{pB} = 37.761^\circ$ .

For small PBAs,  $\phi_{pB} \leq 5^\circ$ , the upper limit on  $|\epsilon|$  is calculated from  $\ell$  of Eq. (4),  $|\epsilon| = \ell \leq 0.0153$ , and represents the domain of so-called epsilon-near-zero (ENZ) materials [16].

Negative real values of  $\epsilon$  at  $\theta = 180^\circ$  [14] are given by

$$\epsilon = \epsilon_r = -\frac{1}{2} \tan^2 \phi_{pB} [1 + (9 - 8 \sin^2 \phi_{pB})^{1/2}] \quad (6)$$

and represent light reflection at an ideal dielectric–plasmonic medium interface. The corresponding total reflection phase shift  $\delta_p$  as  $\theta \rightarrow 180^\circ$  (at the end point of each contour in Fig. 1)

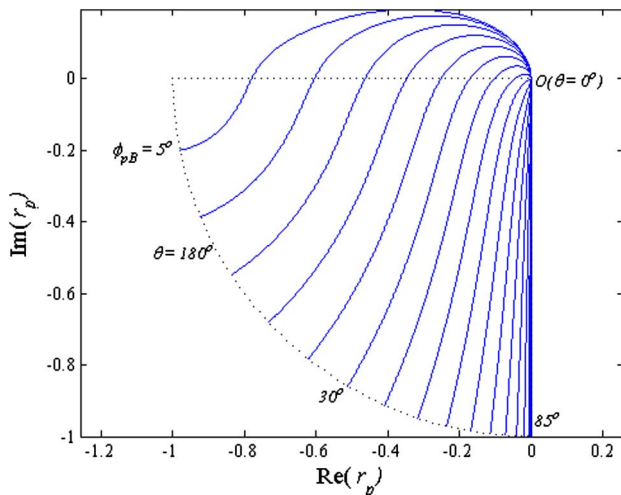


Fig. 1. Complex-plane trajectories of  $r_p$  at discrete values of the PBA  $\phi_{pB}$  from  $5^\circ$  to  $85^\circ$  in equal steps of  $5^\circ$  as  $\theta = -\arg(\epsilon)$  covers the full range  $0^\circ \leq \theta \leq 180^\circ$ .

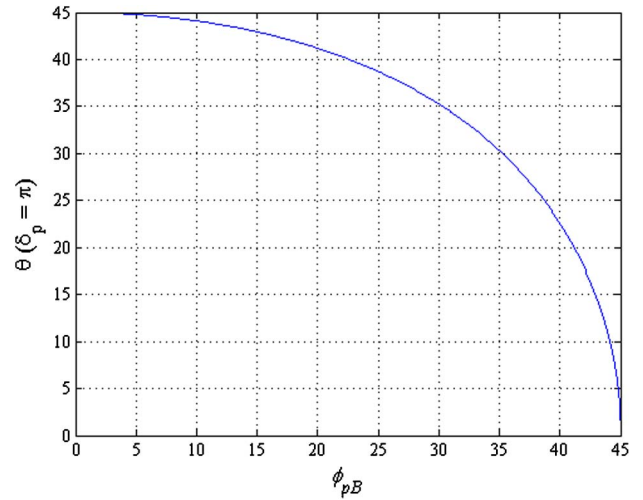


Fig. 2. Graph of the function of Eq. (5). Both  $\phi_{pB}$  and  $\theta$  are in degrees.

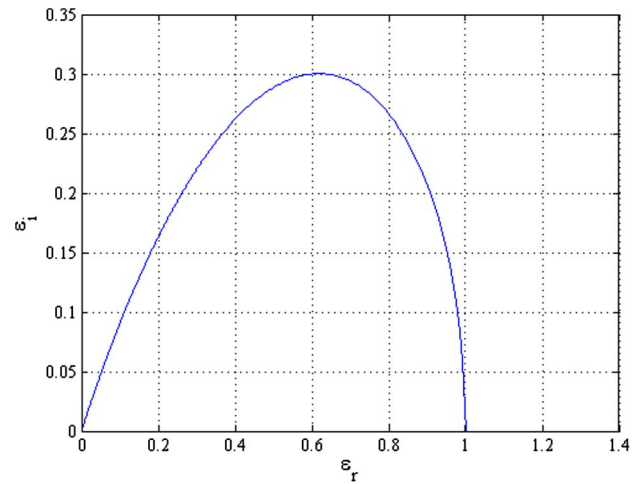


Fig. 3. Locus of all possible values of complex  $\epsilon$  such that  $\delta_p = \arg(r_p) = \pi$  at the PBA.

is obtained from Eqs. (1) and (6) and is plotted as a function of  $\phi_{pB}$  in Fig. 4. In Fig. 4  $\delta_p$  increases monotonically from  $-180^\circ$  to  $-90^\circ$  as  $\phi_{pB}$  increases from  $0^\circ$  to  $90^\circ$ . The initial rise of  $\delta_p$  with respect to  $\phi_{pB}$  is linear for  $\phi_{pB} < 20^\circ$  and then transitions to saturation at  $\phi_{pB} > 70^\circ$ , in accord with Fig. 1.

In Fig. 5  $\delta_p$  is plotted as a function of  $\theta$  for  $\phi_{pB}$  from  $10^\circ$  to  $40^\circ$  in equal steps of  $10^\circ$ . Vertical transitions from  $+180^\circ$  to  $-180^\circ$  are located at  $\theta$  values that agree with Eq. (5).

Another family of  $\delta_p$ -versus- $\theta$  curves for  $\phi_{pB}$  from  $45^\circ$  to  $85^\circ$  in equal steps of  $5^\circ$  is shown in Fig. 6. For  $\phi_{pB} > 45^\circ$  the  $\delta_p$ -versus- $\theta$  curve first exhibits a minimum then reaches saturation as  $\theta \rightarrow 180^\circ$ . The saturated value of  $\delta_p$  is a function of  $\phi_{pB}$  and is shown in Fig. 4.

## 3. COMPLEX REFLECTION COEFFICIENT OF THE *s* POLARIZATION AT THE PBA

Figure 7 shows the loci of complex  $r_s$  as  $\theta$  increases from  $0^\circ$  to  $180^\circ$  at discrete values of  $\phi_{pB}$  from  $5^\circ$  to  $85^\circ$  in equal steps of  $5^\circ$ . All curves start on the real axis at  $\theta = 0$ ,  $r_s = \cos(2\phi_{pB})$ , which is the *s* amplitude reflectance at the Brewster angle of a

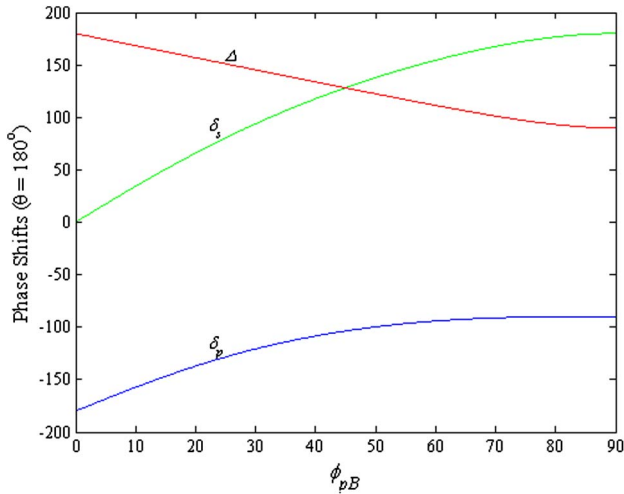


Fig. 4. Total reflection phase shifts  $\delta_p$ ,  $\delta_s$ , and  $\Delta = \delta_p - \delta_s + 360^\circ$  at the interface between a dielectric and plasmonic medium in the limit as  $\theta \rightarrow 180^\circ$  ( $\epsilon_i = 0, \epsilon_r < 0$ ) are plotted as a functions of  $\phi_{pB}$ . All angles are in degrees.

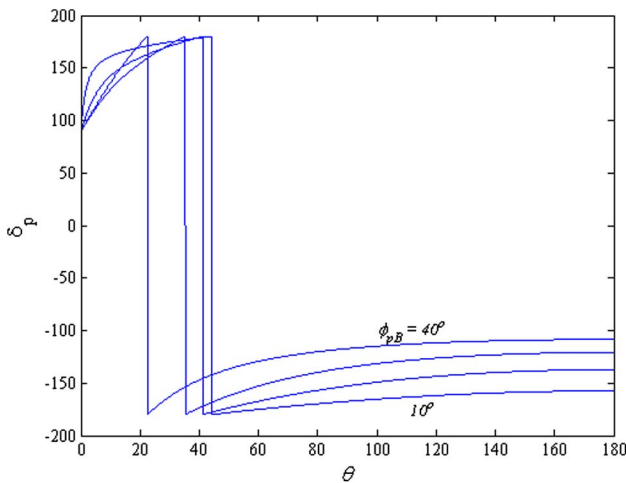


Fig. 5. Family of  $\delta_p$  versus  $\theta$  curves for  $\phi_{pB}$  from  $10^\circ$  to  $40^\circ$  in equal steps of  $10^\circ$ . Both  $\theta$  and  $\delta_p$  are in degrees.

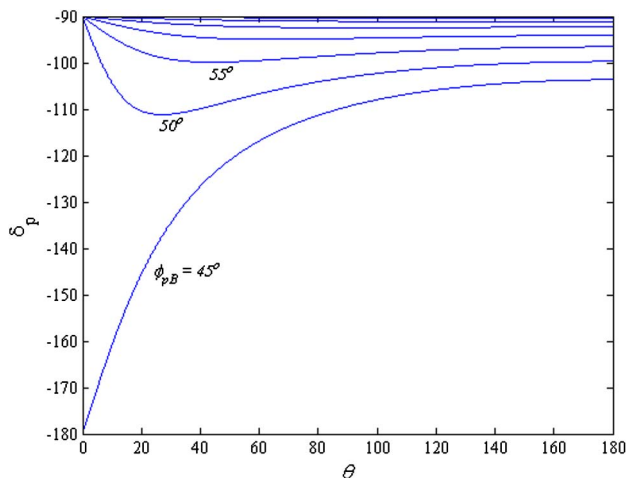


Fig. 6. Family of  $\delta_p$  versus  $\theta$  curves for  $\phi_{pB}$  from  $45^\circ$  to  $85^\circ$  in equal steps of  $5^\circ$ . Both  $\theta$  and  $\delta_p$  are in degrees.

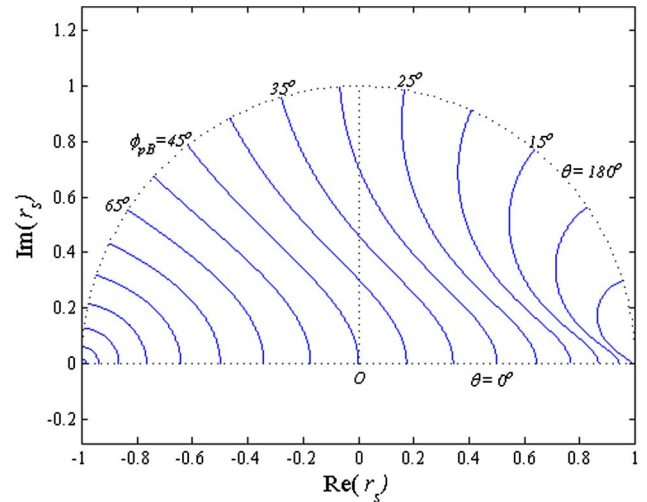


Fig. 7. Complex-plane contours of  $r_s$  at discrete values of the PBA  $\phi_{pB}$  from  $5^\circ$  to  $85^\circ$  in equal steps of  $5^\circ$  as  $\theta = -\arg(\epsilon)$  covers the full range from  $0^\circ$  to  $180^\circ$ .

dielectric–dielectric interface [17], and terminate on the upper half of the unit circle (dotted line) that represents total reflection  $r_s = \exp(j\delta_s)$  at  $\theta = 180^\circ$  ( $\epsilon_i = 0, \epsilon_r < 0$ ). The associated total reflection phase shift  $\delta_s$  along the dotted semicircle is a function of  $\phi_{pB}$  as shown in Fig. 4.

Although we are locked on the PBA, all possible values of complex  $r_s$  (within the upper half of the unit circle) are generated at that angle. This is not the case of complex  $r_p$  at the PBA (Fig. 1) which is squeezed mostly in the third quadrant of the unit circle. Recall that the unconstrained domain of  $r_p$  for light reflection at all dielectric–conductor interfaces is on and inside the full unit circle [17].

#### 4. RATIO OF COMPLEX REFLECTION COEFFICIENTS OF THE $p$ AND $s$ POLARIZATIONS AT THE PBA

The ratio of complex  $p$  and  $s$  reflection coefficients, also known as the ellipsometric function  $\rho = \tan \psi \exp(j\Delta)$  [13], is obtained from Eqs. (1) and (2) as

$$\rho = r_p/r_s = \frac{\sin \phi \tan \phi - (\epsilon - \sin^2 \phi)^{1/2}}{\sin \phi \tan \phi + (\epsilon - \sin^2 \phi)^{1/2}}. \quad (7)$$

Figure 8 shows loci of complex  $\rho$  as  $\theta$  increases from  $0^\circ$  to  $180^\circ$  at constant values of  $\phi_{pB}$  from  $5^\circ$  to  $85^\circ$  in equal steps of  $5^\circ$ . All contours begin at the origin  $O$  (as a common point that represents the ideal Brewster-angle condition of  $r_p = 0$  at  $\theta = 0$ ), then fan out and terminate on the  $90^\circ$  arc of the unit circle in the second quadrant of the complex plane (dotted line), so that  $\rho = \exp(j\Delta)$  at  $\theta = 180^\circ$  ( $\epsilon_i = 0, \epsilon_r < 0$ ). The differential reflection phase shift  $\Delta = \delta_p - \delta_s + 360^\circ$  at  $\theta = 180^\circ$  decreases monotonically from  $180^\circ$  to  $90^\circ$  as  $\phi_{pB}$  increases from  $0^\circ$  to  $90^\circ$  as shown in Fig. 4.

#### 5. SUMMARY

The Fresnel complex reflection coefficients  $r_p$ ,  $r_s$  and their ratio  $\rho = r_p/r_s$  are evaluated at the PBA  $\phi_{pB}$  of a dielectric–conductor interface for all possible values of the complex relative dielectric function  $\epsilon = |\epsilon| \exp(-j\theta) = \epsilon_r - j\epsilon_i$ ,  $\epsilon_i > 0$ .

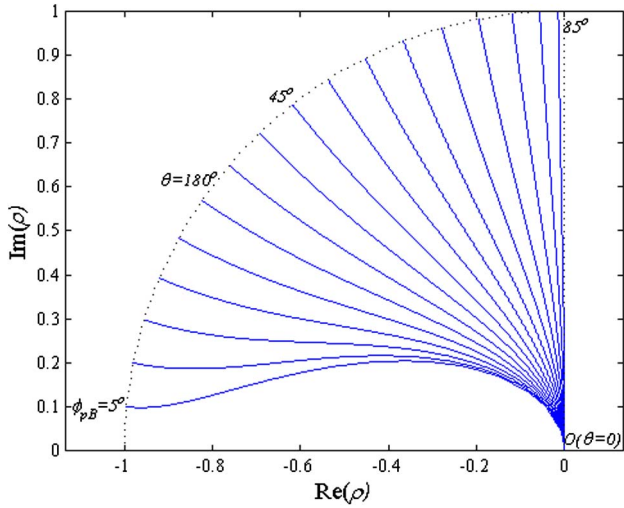


Fig. 8. Complex-plane trajectories of the ratio  $\rho = r_p/r_s$  at discrete values of the PBA  $\phi_{pB}$  from  $5^\circ$  to  $85^\circ$  in equal steps of  $5^\circ$  as  $\theta = -\arg(\epsilon)$  covers the full range  $0^\circ \leq \theta \leq 180^\circ$ .

Complex-plane loci of  $r_p$ ,  $r_s$ , and  $\rho$  at the PBA are obtained at discrete values of  $\phi_{pB}$  from  $5^\circ$  to  $85^\circ$  in equal steps of  $5^\circ$  and as  $\theta$  increases from  $0^\circ$  to  $180^\circ$ ; these are presented in Figs. 1, 7, and 8, respectively. The reflection phase shift  $\delta_p$  of the  $p$  polarization at the PBA is plotted as function of  $\theta$  in Figs. 5 and 6 for two different sets of  $\phi_{pB}$ . For  $\phi_{pB} > 70^\circ$  (e.g., high-reflectance metals in the IR),  $r_p$  at the PBA is essentially pure negative imaginary and  $\delta_p = \arg(r_p) \approx -90^\circ$ . In the domain of fractional optical constants (vacuum UV or light incidence from a high-refractive-index immersion medium)  $0^\circ < \phi_{pB} < 45^\circ$ , and  $r_p$  is pure real negative ( $\delta_p = \pi$ ) at  $\theta = \tan^{-1}(\sqrt{\cos(2\phi_{pB})})$ . The associated locus of complex  $\epsilon$  is shown in Fig. 3. Finally, the total reflection phase shifts  $\delta_p$ ,  $\delta_s$ ,  $\Delta = \arg(\rho)$  at an ideal dielectric–plasmonic medium interface ( $\epsilon_i = 0$ ,  $\epsilon_r < 0$ ), are shown as functions of  $\phi_{pB}$  in Fig. 4.

## APPENDIX A

By setting  $\epsilon_r = x$  and  $\epsilon_i = y$ , the Cartesian equation of a constant- $\phi_{pB}$  contour (a cardioid [8]) takes the form [10]

$$y^2 = a + (a^2 - bx)^{1/2} - x^2, \quad (\text{A1})$$

$$a = u^2(1.5 - u)/(1 - u)^2, b = u^3/(1 - u)^2, u = \sin^2 \phi_{pB}. \quad (\text{A2})$$

The locus of complex  $\epsilon$  such that  $\delta_p = \arg(r_p) = \pi$  at a given angle of incidence  $\phi = \sin^{-1}\sqrt{u}$  is a circle [18]

$$y^2 = 2ux - x^2. \quad (\text{A3})$$

Equations (A1) and (A3) are satisfied simultaneously if their right-hand sides are equal; this gives

$$(a^2 - bx)^{1/2} = 2ux - a. \quad (\text{A4})$$

By squaring both sides of Eq. (A4) we obtain

$$4u^2x^2 = (4au - b)x. \quad (\text{A5})$$

Equation (A5) is obviously satisfied when  $x = 0$ , and from Eq. (A3) one gets  $y = 0$  and  $\epsilon = 0$ . The more significant solution of Eq. (A5) is

$$x = (4au - b)/(4u^2). \quad (\text{A6})$$

Substitution of  $a$  and  $b$  from Eq. (A2) in Eq. (A6) leads to the simple result

$$x = u/(1 - u). \quad (\text{A7})$$

The associated value of  $y$  is then obtained from Eq. (A3) as

$$y = u\sqrt{1 - 2u}/(1 - u). \quad (\text{A8})$$

The angle  $\theta = \arg(\epsilon)$  is determined from Eqs. (A7) and (A8) by

$$\tan \theta = y/x = \sqrt{1 - 2u}. \quad (\text{A9})$$

Finally, substitution of  $u = \sin^2 \phi_{pB}$  in Eq. (A9) gives

$$\theta(\delta_p = \pi) = \tan^{-1}\left(\sqrt{\cos(2\phi_{pB})}\right). \quad (\text{A10})$$

This completes the proof of Eq. (5).

## REFERENCES

1. S. P. F. Humphreys-Owen, "Comparison of reflection methods for measuring optical constants without polarimetric analysis, and proposal for new methods based on the Brewster angle," *Proc. Phys. Soc. London* **77**, 949–957 (1961).
2. H. B. Holl, "Specular reflection and characteristics of reflected light," *J. Opt. Soc. Am.* **57**, 683–690 (1967).
3. G. P. Ohman, "The pseudo-Brewster angle," *IEEE Trans. Antennas Propag.* **25**, 903–904 (1977).
4. R. M. A. Azzam, "Maximum minimum reflectance of parallel-polarized light at interfaces between transparent and absorbing media," *J. Opt. Soc. Am.* **73**, 959–962 (1983).
5. S. Y. Kim and K. Vedam, "Analytic solution of the pseudo-Brewster angle," *J. Opt. Soc. Am. A* **3**, 1772–1773 (1986).
6. T. E. Darcie and M. S. Whalen, "Determination of optical constants using pseudo-Brewster angle and normal-incidence reflectance," *Appl. Opt.* **23**, 1130–1131 (1984).
7. Y. Lu and A. Penzkofer, "Optical constants measurements of strongly absorbing media," *Appl. Opt.* **25**, 221–225 (1986).
8. R. M. A. Azzam and E. Ugbo, "Contours of constant pseudo-Brewster angle in the complex  $\epsilon$  plane and an analytical method for the determination of optical constants," *Appl. Opt.* **28**, 5222–5228 (1989).
9. M. A. Ali, J. Moghaddasi, and S. A. Ahmed, "Optical properties of cooled rhodamine B in ethanol," *J. Opt. Soc. Am. B* **8**, 1807–1810 (1991).
10. R. M. A. Azzam, "Analytical determination of the complex dielectric function of an absorbing medium from two angles of incidence of minimum parallel reflectance," *J. Opt. Soc. Am. A* **6**, 1213–1216 (1989).
11. I. H. Campbell and P. M. Fauchet, "Temporal reshaping of ultrashort laser pulses after reflection from GaAs at Brewster's angle," *Opt. Lett.* **13**, 634–636 (1988).
12. Y. Lv, Z. Wang, Y. Jin, M. Cao, L. Han, P. Zhang, H. Li, H. Gao, and F. Li, "Spin polarization separation of light reflected at Brewster angle," *Opt. Lett.* **37**, 984–986 (2012).
13. R. M. A. Azzam and N. M. Bashara, *Ellipsometry and Polarized Light* (North-Holland, 1987).
14. R. M. A. Azzam and A. Alsamman, "Plurality of principal angles for a given pseudo-Brewster angle when polarized light is reflected at a dielectric-conductor interface," *J. Opt. Soc. Am. A* **25**, 2858–2864 (2008).

15. R. M. A. Azzam and E. Ugbo, "Angular range for reflection of  $p$ -polarized light at the surface of an absorbing medium with reflectance below that at normal incidence," *J. Opt. Soc. Am. A* **19**, 112–115 (2002).
16. A. Alù, M. G. Silveirinha, A. Salandrino, and N. Engheta, "Epsilon-near-zero metamaterials and electromagnetic sources: tailoring the radiation phase pattern," *Phys. Rev. B* **75**, 155410 (2007).
17. R. M. A. Azzam, "Direct relation between Fresnel's interface reflection coefficients for the parallel and perpendicular polarizations," *J. Opt. Soc. Am.* **69**, 1007–1016 (1979).
18. R. M. A. Azzam, "Reflection of an electromagnetic plane wave with 0 or  $\pi$  phase shift at the surface of an absorbing medium," *J. Opt. Soc. Am.* **69**, 487–488 (1979).